Three-Dimensional Printing of Super-Resolution Microscopy Images

Emily M. Mace,[1]* Jesse Moon,[2] and Jordan S. Orange[1]

[1]Center for Human Immunobiology, Texas Children's Hospital and Baylor College of Medicine, Houston, TX 77030

[2]Freelance Industrial Designer, Austin, TX

*mace@bcm.edu

Introduction

Human beings are tactile creatures, and the ability to handle and observe an object from multiple dimensions is a powerful tool for us. As microscopists we often extract quantitative data from the reconstructions of cellular structures observed in micrographs. Within the past 200 years, technology has exploded at such a rate that we now have the ability to visualize subcellular features with resolution that is no longer limited by the diffraction barrier of light, and we are able to resolve complex structures, sometimes with double-digit nanometer resolution. In addition, time-resolved imaging in three dimensions is increasingly feasible and informative.

Recently the commercialization of desktop three-dimensional (3D) printers has provided opportunities for institutions and businesses to exploit this technology. It is now in the hands of scientists and medical doctors for use in the bioengineering and medical fields. Cell biology is no exception. With the ability to model cellular structures, we are able to more fully enter the world that holds us so fascinated. While the uses of 3D printing and nanofabrication for bioengineering purposes are extensive, this article will specifically describe the use of 3D printing to model non-diffraction-limited stimulated emission depletion (STED) microscopy images [1, 2].

Materials and Methods

Printers. 3D printers are available in a range of prices and features. These are dictated in part by the technologies used: stereolithography, fused deposition modeling, selective laser sintering, selective laser melting, electron beam melting, and laminated object manufacturing (a comprehensive review of 3D printing technology can be found at http://3dprintingindustry.com/3d-printing-basics-free-beginners-guide/technology). Most of the entry-level consumer models are based on the fused deposition modeling principle, in which thermoplastics are melted and deposited using Cartesian coordinate (*X*,*Y*,*Z*) driven motors to convert a 3D computer graphics model into a printed object. In this case we have used a MakerBot® Replicator 2X, in which the *XY* stage is fixed and the extruders move in the *XYZ* plane to deposit filament. This requires the rendering of the 3D image into a suitable file format and subsequently importing it into the MakerBot software (Makerware), followed by printing with acrylonitrile butadiene styrene (ABS) filament.

Natural killer cells. Our purpose was to model the F-actin cytoskeleton of natural killer (NK) cells [3]. NK cells are innate immune effector cells that recognize and kill virally infected and tumorigenic targets. As such, they are a critical component of human host defense [4]. Their deadly yet specific function relies on the directed secretion of specialized lysosomes, termed lytic granules, which contain perforin and granzymes. These lytic granules, which range in size from 100–750 nm, are secreted through clearances in a pervasive F-actin network at the immunological synapse formed between the NK cell and its target [5, 6]. The regulation of F-actin is an important area of interest in the cell biology of this specialized type of secretion. In order to study the structure and regulation of F-actin, we used a technique in which we activated NK cells on glass coated with antibody to activating receptors (NKp30 and CD18), which induces F-actin rearrangement and ultimately lytic granule degranulation. Cells were fixed, permeabilized, and stained with phalloidin Alexa Fluor 488 to visualize the F-actin. STED microscopy was done on a Leica SP8 STED, with tunable pulsed white light laser and HyD detectors. Images were acquired using LASAF software and deconvolved using Huygens software (Scientific Volume Imaging), which resulted in a final resolution of 40 nm in the *XY* planes and ~200 nm in the *Z* plane.

Results

Following acquisition of the microscopy image and deconvolution with Huygens, we imported the 3D image as .ICS and .IDS files to Imaris 7.4 (Bitplane). In Imaris, we used the surfaces feature to convert the raw data to a computer-generated

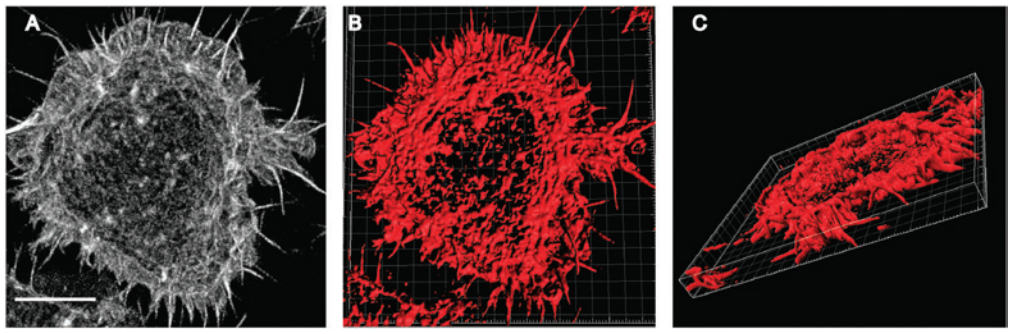

Figure 1: Surface rendering of a STED microscopy image of F-actin in a human NK cell. Images were acquired in *XYZ* on a Leica SP8 STED microscope and subsequently exported to Huygens software for deconvolution (A). Following deconvolution, images were surface rendered in Imaris (Bitplane) (B, C). Scale bar=5 μm.

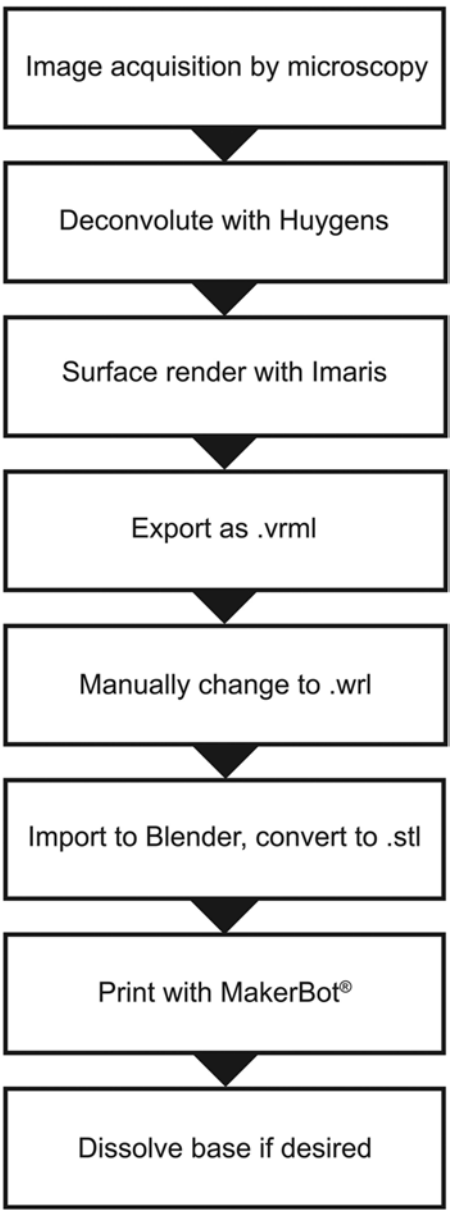

Figure 2: Workflow of file conversion and processing from microscopy images to 3D printed model. See text for details.

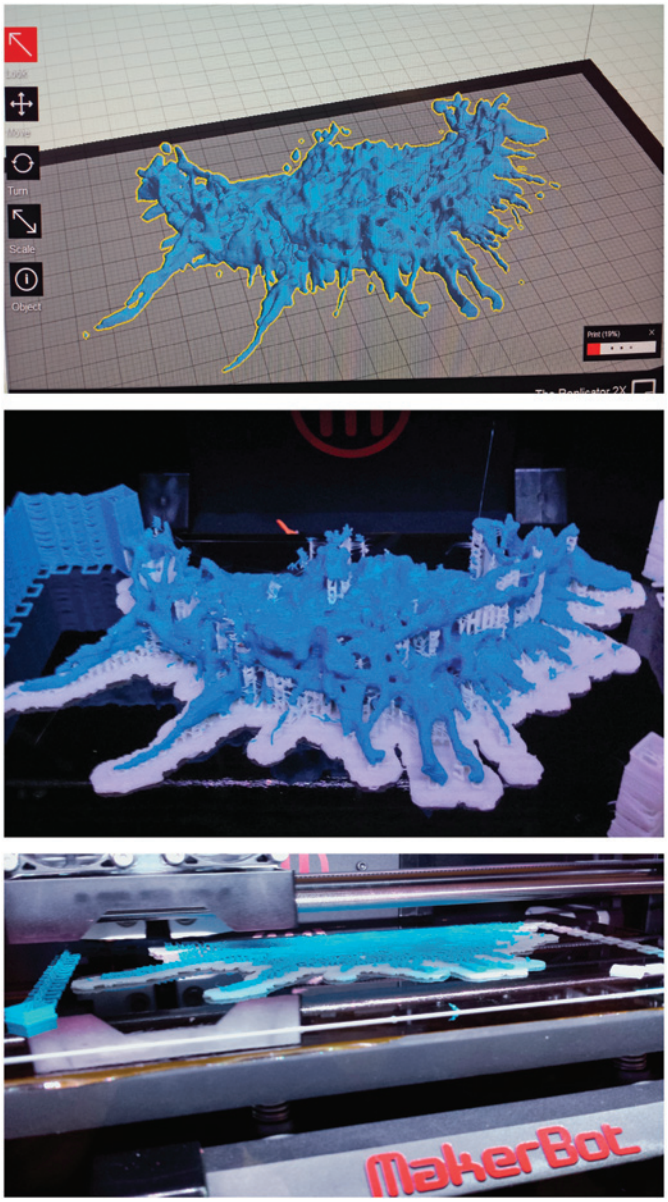

Figure 3: Image rendering in MakerBot software and the printing process. Half the F-actin model is shown, both rendered in software prior to printing and during the print procedure. The model shown is printed with ABS filament for F-actin (blue) and dissolvable filament for the base (white).

representation of our image (Figure 1). This also allowed us to specifically tailor the amount of detail (and consequently the file size) of the rendered object. Files were exported from Imaris as .vrml files, and the file extension was manually changed to .wrl to facilitate import into the open-sourced software Blender (blender.org). Blender was then used to convert the file to the required .stl format for import into the Makerware. Figure 2 shows a flowchart of this workflow.

Following import into Makerware, the image was appropriately sized for printing. For one continuous run we limited the printed diameter to approximately 10 cm. When larger models were made, we divided these into 2 halves or 4 quarters to allow each piece to be printed individually (an example of a halved model is shown in Figure 3). In order to print the detail of the F-actin filaments, which includes spider-like protrusions, the printed image was generated on a base that includes filler to support these elements. Although early iterations of our model included this base in a neutral color distinct from our F-actin structures, we later used dissolvable filament to first generate the support base, which was subsequently dissolved away. Dissolvable filament is similar to the ABS filament used elsewhere in our design but dissolves in D-limonene (Sigma), a non-toxic, citrus-scented solvent. The MakerBot Replicator 2X has dual extruders, so for our model we printed the F-actin structure with one extruder and the dissolvable base and supports with the second. The printing process itself took approximately 2 hours and, although supervision was required, was usually error-free. Printing was done at standard speed (90 mm/s extrusion speed, 150 mm/s travel speed), at 255°C for the dissolvable filament and 233°C for the ABS filament. Dissolution of the

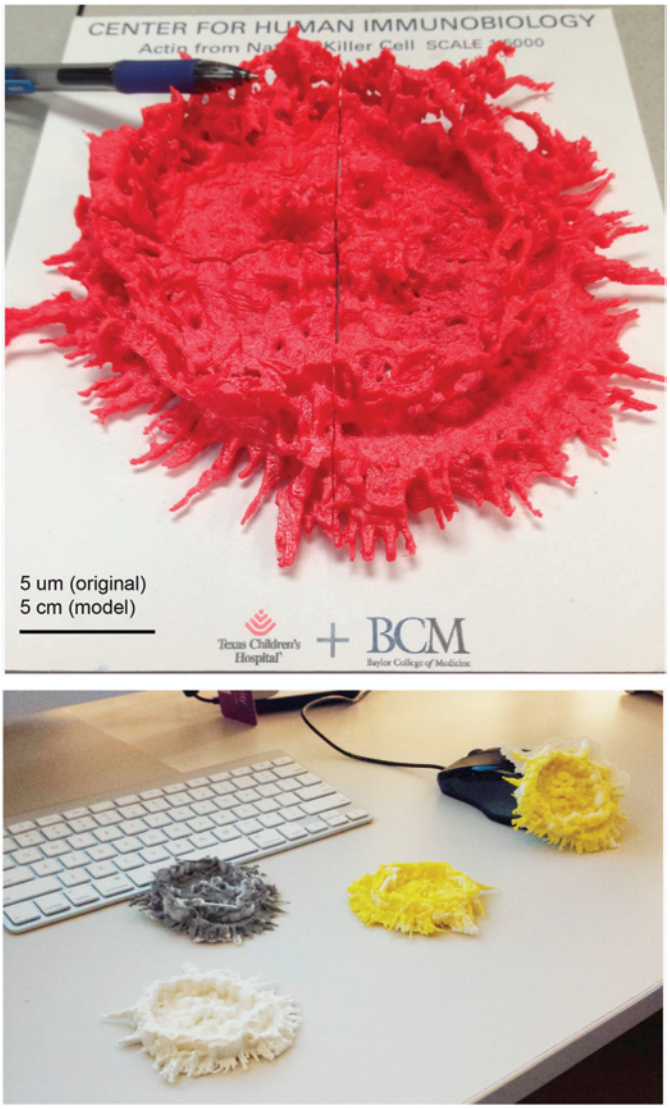

Figure 4: Completed F-actin models: the larger 20 cm model was printed in quarters (top), and the 10 cm models were printed in various colors (bottom). Scale bar (top)=5 cm on model; scale bar=5 µm on original STED image.

base required a three-hour session in a 2L D-limonene bath, followed by cleaning with soap and water to reduce the fairly oily (yet pleasantly scented) residue left by limonene. The final result was a sturdy yet detailed model of the NK cell F-actin cytoskeleton (Figure 4).

Discussion

The greatest troubleshooting aspect of this procedure was the generation of files that were not too complex, particularly given the nature of the cytoskeleton our model was based on. Despite this, we estimate that our printed model gives a resolution of 75 nm at its most detailed points, particularly the actin filaments extending from the cell edge. Rendering at both the Imaris and Blender stages was prone to freezing and crashing our relatively high-powered PC computers if too much detail was retained in the image. In addition, although we had few problems with ABS filament material, switching to polylactic acid (PLA) polymer in an attempt to use opaque-colored filament as a base required significant optimization of extruder head temperature. Ultimately we were unable to find a temperature that sustained printing over the time required without clogging or stopping altogether. This led us to the dissolvable filament, which was much more tractable. Interestingly, we also had varying degrees of success with different colors of ABS filament, certain colors being much more prone to clog than others. Finally, the conversion of multiple file types proved troublesome. While none of the currently available image processing and acquisition software packages offer an .stl file format export option, we are optimistic that with the rise in popularity of 3D printing, this is not far off.

In accordance with the open spirit of many of the maker communities, there are a number of openly accessible repositories for 3D print files. These include the MakerBot Thingiverse, which features more than 400,000 designs (thingiverse.com). With specific scientific focus, the NIH 3D print exchange (http://3dprint.nih.gov) was launched in June 2014 in order to coincide with the first White House Maker Faire. The site offers a repository for models and laboratory equipment, as well as instructional videos and a discussion forum. In order to share our design with others, the .stl files comprising our large actin model were deposited on the NIH 3D print exchange website and are available at http://3dprint.nih.gov/discover/3dpx-000748.

Conclusion

The current boom in 3D printing technology is giving rise to a number of creative and innovative applications. The ability to feel the structures that we see in a micrograph is more than a cute exercise. It provides us the ability to add a tactile component to our thinking about the cell structures and biological processes in which we are engaged. Further, it provides a touchstone through which we can share our research and engage the public. As researchers working in a clinical setting, this provides an important way to bring the seemingly intangible ideas of immune function to those who are not immunologists or cell biologists. This could include a powerful experience for the blind or the visually impaired. Through our combination of non-diffraction limited microscopy with 3D printing, we have made small cell structures not just visible, but also touchable.

Acknowledgments

The authors wish to thank Dr. T. Feinstein for the initial dialogue that led to this article. This work is supported by the 3D Print Program of the Center for Human Immunobiology at Texas Children's Hospital.

References

[1] D Toomre and J Bewersdorf, *Annu Rev Cell Dev Biol* 26 (2010) 285–314.
[2] EM Mace and JS Orange, *Front Immunol* 3 (2012) 421.
[3] K Lagrue et al., *Immunol Rev* 256(1) (2013) 203–21.
[4] JS Orange, *J Allergy Clin Immunol* 132(3) (2013) 515–25, quiz 526.
[5] GD Rak et al., *PLoS Biol* 9(9) (2011) e1001151.
[6] AC Brown et al., *PLoS Biol* 9(9) (2011) e1001152.

MT